Experimental Characterisation of the Novel HALO Plasma Thruster for Small Satellite Applications

Conference Paper · March 2021

CITATIONS
9

READS
958

6 authors, including:

Silvia Masillo
University of Surrey
16 PUBLICATIONS **83** CITATIONS
SEE PROFILE

Burak Karadag
Debye Ltd
45 PUBLICATIONS **271** CITATIONS
SEE PROFILE

Aaron Knoll
Imperial College London
122 PUBLICATIONS **1,130** CITATIONS
SEE PROFILE

Paolo Bianco
Forschungszentrum Jülich
11 PUBLICATIONS **70** CITATIONS
SEE PROFILE

EXPERIMENTAL CHARACTERISATION OF THE NOVEL HALO PLASMA THRUSTER FOR SMALL SATELLITE APPLICATIONS

SPACE PROPULSION 2020+1
17 – 18 – 19 MARCH 2021

Silvia Masillo [(1)], Andrea Lucca Fabris [(2)], Burak Karadag [(3)], Thomas Potterton [(4)], Aaron Knoll [(5)], Paolo Bianco [(6)]

[(1)] Surrey Space Centre, University of Surrey, Guildford (United Kingdom), Email: s.masillo@surrey.ac.uk
[(2)] Surrey Space Centre, University of Surrey, Guildford (United Kingdom), Email: a.luccafabris@surrey.ac.uk
[(3)] Surrey Space Centre, University of Surrey, Guildford (United Kingdom), Email: b.karadag@surrey.ac.uk
[(4)] Surrey Satellite Technology Ltd, Guildford (United Kingdom), Email: t.potterton@sstl.co.uk
[(5)] Imperial College London, London (United Kingdom), Email: a.knoll@imperial.ac.uk
[(6)] Airbus Defence and Space, Portsmouth (United Kingdom), Email: paolo.bianco@airbus.com

KEYWORDS: Electric propulsion, Hall Effect, Cylindrical Hall thruster, Hollow cathode neutraliser.

ABSTRACT:

The Halo thruster is currently under investigation within Surrey Space Centre, at the University of Surrey, in a collaboration with Airbus Defence and Space, Surrey Satellite Technology Ltd and Imperial College London to address the growing market need for low-cost and low-power small satellite propulsion systems. This paper presents an overview of the experimental setup of the novel Halo thruster and compares performance data between different thruster configurations. The forthcoming test campaign is going to focus on plasma investigation - ion beam current, ion energy and charge diagnostic by Faraday probe and Wien filter, Optical Emission Spectroscopy and discharge waveform oscillations data – and performance optimisation. The design of an in-house developed hollow cathode neutralizer is also presented. For the thruster configuration presented in this paper, the cathode is encased in the Halo thruster cylindrical discharge channel with its axis aligned to the thruster centreline.

1. INTRODUCTION

In the last decade, efforts towards lowering the cost of access to space have led to a rapidly increasing interest for small satellites and, consequently, to the necessity to design mass and power-limited subsystems. In this framework, novel Electric Propulsion (EP) technologies are being developed to offer low cost solutions which can satisfy low power requirements of the small satellite industry.
Because of their relatively high efficiency at moderately high specific impulse, Hall accelerators are, at present, the most commonly used plasma thrusters. Annular Hall Effect Thrusters (HETs) have a noteworthy flight heritage but scale poorly in efficiency at the low power level of small satellites (<500 kg and order of ~100-200 W), as a result of increased wall losses and magnetic circuit overheating with decreasing size. Consequently, unconventional HET concepts have been developed, such as Cylindrical Hall thrusters (CHTs) [1], Cusped Field Thrusters (CFTs) [2] and External Discharge Plasma Thruster (XPT) [3] which feature an improved efficiency at low power, a reduced surface-to-volume ratio in comparison to annular HETs and, potentially, a reduced channel erosion and higher ionisation efficiency.
The Halo thruster (Figure 1), developed at the Surrey Space Centre (SSC) since 2010, has demonstrated efficiencies at low power comparable to the state-of-art annular HETs of commensurate size, CHTs and CFTs [4]. Aiming to work more efficiently at low power conditions, the Halo thruster is designed with a cylindrical discharge channel and a cusped magnetic field topology, which creates regions of magnetic field cancellation in two locations: a null point at the centre of the discharge channel exit, and an annular region in front of the anode. This B-field topology has been conceived to promote electron confinement, to reduce wall losses, to decrease the beam divergence, as well as to enable advanced engineering solutions such as using of a centrally-located cathode. The latest produces a stream of electrons to sustain the plasma within the discharge channel and to neutralize the ejected ion beam. Within the discharge channel, electrons are trapped in a closed-loop azimuthal drift sustained by the combination of electric and magnetic fields, impeding the local electron axial transport. As a consequence of the reduced electron axial mobility, a local electric field is established which accelerates the ions downstream with high exhaust velocity. A novel Halo thruster design takes advantage of the high magnetic field, provided at small scale by SmCo permanent magnets (PMs), and the integration of an in-house designed hollow cathode at the centre

of the thruster enabling the use of all propellant in the main plasma discharge [5].
The experimental activities, previously planned for 2020 and postponed to Spring 2021 due to the COVID-19 pandemic, include plasma investigations (ion beam current, ion energy and charge by Faraday probe and ExB probes, along with Optical Emission Spectroscopy (OES) and discharge waveform oscillations data) and performance optimisation related to different power levels, changes in the cathode position and propellant mass flow rates. In this paper, a new experimental setup for a novel prototype of Halo is introduced. Moreover, a comparison of performance measurements, based on Halo thruster previous testing campaigns, is presented, considering a broad range of operating condition and configurations.

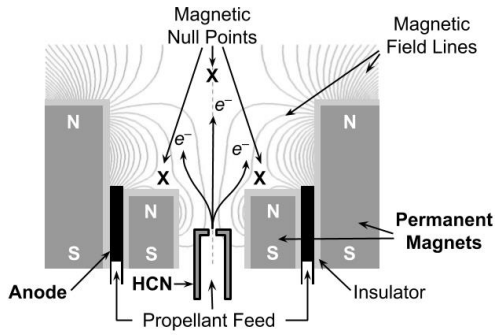

Figure 1. Schematic of the Halo Thruster concept with the use of PMs and a centrally-located cathode.

2. PERMANENT MAGNET HALO THRUSTER

The Halo project started in 2010, merging the experiences in EP system development from SSC, Airbus Defence and Space, Surrey Satellite Technology Limited (SSTL) and Imperial College London (ICL). During multiple technology development iterations, different prototypes of the thruster were developed, which share a similar magnetic field configuration and mostly differ for the magnetic means (PM or electromagnets (EM)), neutraliser location and discharge channel dimensions. Experimental results and plasma diagnostic measurements of the different Halo configurations can be found in previous publications [4-6]. The first PM Halo design included Neodymium-Iron-Boron (NdFeB) magnets. However, the low temperature tolerance of the NdFeB magnets imposed a limit on the short time in which the thruster could safely operate.
In this paper, a novel PM Halo design is described: Halo is renewed with SmCo magnets and an updated mass flow feed system. Moreover, the design includes an in-house developed hollow cathode neutraliser (HCN). The cathode, named OSMO and described in Sec.3, is located at the bottom end of the discharge channel with its axis aligned to the thruster centreline enabling propellant recovery. As shown in a cutaway view of the Halo thruster in in Figure 2, the main components of the thruster are: a cylindrical channel made of Boron Nitride (BN); a copper anode, characterised by an annular internal cavity with a diameter of 42mm, which is positively biased and serves also as gas distributor; propellant lines designed to feed the propellant radially from an inlet within the annular section of the thruster on the outer discharge channel wall; copper heat sink, with optional water cooling, at the rear of the thruster; two concentrically aligned SmCo annular PMs of grade XG24/25; an external case whose dimensions are 84mm at the outer diameter and a length of 88mm. The SmCo magnets were selected for the strong maximum energy density product and high coercivity. These PMs allowed longer thruster operations, compared with the NdFeB ones, thanks to a working temperature up to 350 °C. Furthermore, in comparison to EM coils of the same dimensions, the SmCo PMs induce a higher B-field intensity without any power consumption. The high B-field strength at small scale should allow better plasma confinement, reducing wall sputtering erosion caused by high-energy ions and decreasing power loss associated to plasma flows to the channel walls. Moreover, the issues caused by excessive heat dissipation of the EM coils are avoided and the thruster design is simplified. The Halo thruster is designed with the PMs aligned with the poles facing in the same direction to generate axisymmetric cusp regions within the discharge channel and the annular halo close to the anode to promote greater electron confinement.

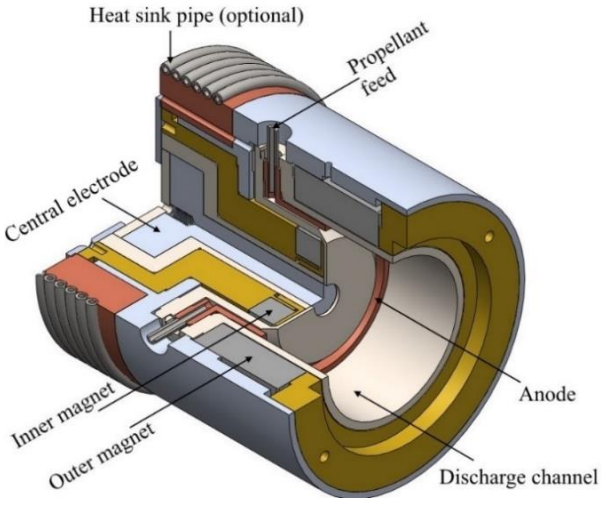

Figure 2. A cutaway view of the Halo thruster 3D CAD.

Figure 3 highlights the B-field flux density, as calculated by Finite Element Method Magnetics (FEMM): the halo is enclosed by a toroidal cusp structure along with a spherical magnetic field cancellation region, which is also enclosed by a cusp structure, along the thruster axis of symmetry downstream the thruster exit. The B-field strength profile is showed as comparison between:
- r=0mm (red line): symmetry axis of the thruster;
- r=11mm (blue): axial path intersecting the halo;
- r=22.5mm (green): axial path starting at the downstream surface of the anode.

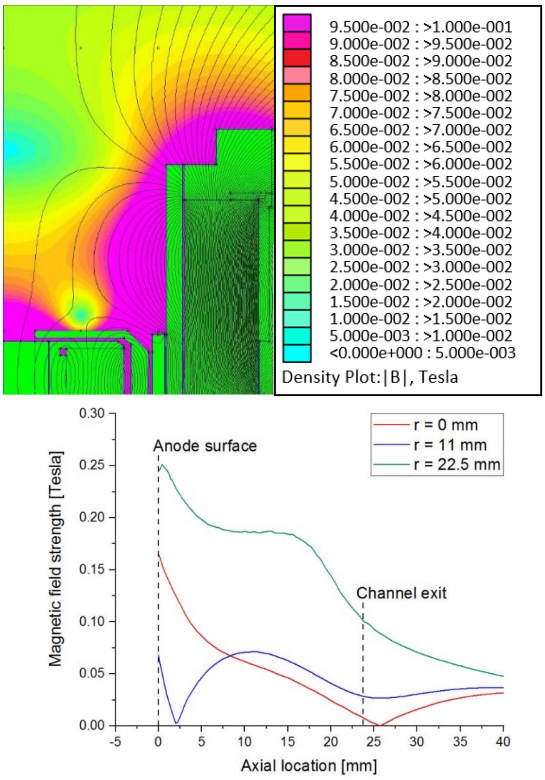

Figure 3. PM Halo thruster B-field circuit model simulated by FEMM and B-field strength profile.

3. OSMO Cathode

The OSMO cathode was designed to be used as a cost-effective neutraliser for ground testing of electric thrusters and will be implemented as Halo thruster neutraliser in the next test campaign. As shown in Figure 2, a 13mm diameter cavity along the symmetry axis of the Halo thruster allows to allocate the electron source.

The OSMO cathode, in Figure 4, is characterized by the following features:

- A lanthanum hexaboride (LaB_6) emitter;
- The molybdenum keeper electrode.

The cathode has a diameter of 26mm and a length of 50mm (measuring from the keeper disc to bottom of the ceramic base).

Although dispenser cathodes, which have a barium-based compound in the pores of a tungsten matrix, are appealing due to their low work function surface for the thermionic electron emission, LaB_6 inserts are more suitable for laboratory environment because of their less sensitivity to poisoning and low evaporation rates.

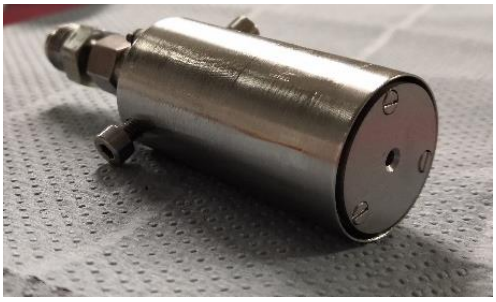

Figure 4. The OSMO cathode assembled at the Surrey Space Centre EP laboratory.

Preliminary tests on the OSMO cathode were carried out in December 2020 at SSC EP Laboratory, University of Surrey. The cathode was ignited by using xenon as propellant and 105W supplied to the heater.

The use of the centrally mounted neutraliser enables the possibility of using the whole propellant supplied to the thruster. In the conventional externally-located cathode configuration, in fact, the neutral flow which exits the cathode discharge is generally considered "lost". Mounting the cathode internally, along the thruster centreline, might potentially reduce plume divergence and increase near-field plume symmetries, thus improve coupling of the cathode plume with the thruster discharge in comparison to the traditional external HCN design. This design allows to keep a low electrostatic potential along the magnetic field line overlapping with thruster centreline and creating a convergent field which might reduce the beam divergence.

4. EXPERIMENTAL SETUP

The PM HALO thruster tests are performed in the Daedalus vacuum chamber at the Surrey Space Centre Electric Propulsion Laboratory, University of Surrey.

4.1. Daedalus Vacuum Chamber

The Daedalus chamber, in Figure 5, has a diameter of 1.5m and a total length of 3m. It is equipped with a three-stage pumping system, incorporating a 660mm cryo-panel (recently added and available in future test campaigns) and two cryogenic pumps in parallel with a turbomolecular pump. The chamber achieves a base pressure in the range of 10^{-7} Torr.

The chamber is also equipped with a variety of feedthroughs and propellant feedlines, thruster power lines, sensor signal lines and a series of viewing ports at different locations around the chamber. Multiple pressure gauges are installed in critical locations along the vacuum system to measure pressure levels in the chamber and pumping lines.

Figure 5. The Daedalus Vacuum Chamber at the Surrey Space Centre.

4.2. Diagnostic System

4.2.1. Thrust Balance

A hanging pendulum-type thrust stand with sub-millinewton resolution is used to take direct thrust measurements. The thrust stand (Figure 6), developed at SSC, has a pendulum-type configuration in which the propulsion system is suspended on movable platform supported by metallic flexures. The thrust generated by the propulsion system produces displacements of the movable platform, which are recorded by a laser displacement sensor. The laser measurement is performed using a Micro-Epsilon model ILD 1700-2 laser sensor, with a linearity of ±0.1% Full Scale Output and a resolution of 0.1 μm. For small displacements, a linear relationship between thrust and the change of position of the movable beam can be established. As Eq.1 states, the displacement l is proportional to the thrust force F:

$$l = F/C \qquad \text{Eq.1}$$

The value of C is the equivalent stiffness of the system and defines the gain factor of the thrust stand. C is determined using a calibration process and it is, hereafter, referred to as the calibration factor.

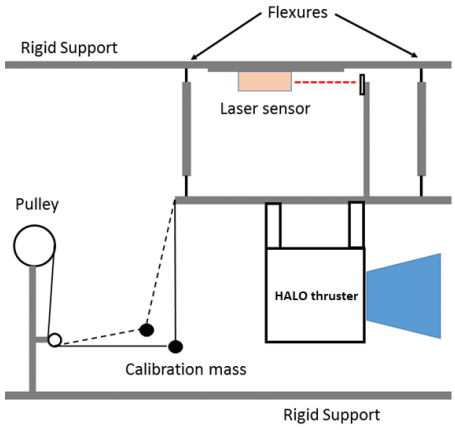

Figure 6. Schematic of the SSC thrust balance.

The calibration process is performed in vacuum conditions with feedlines and power lines already installed to include their inherent stiffness in the resulting calibration factor. Typically, ten force values are used for each calibration run.

The displacement data are processed using a MATLAB code, which applies 5th order Butterworth low-pass filter to the raw data, automatically identifies the displacement steps and performs a linear interpolation of the thrust values versus the displacement to compute the calibration factor. A Monte Carlo algorithm is used to quantify the uncertainty of the calibration factor originating from the uncertainties of mass and geometrical dimensions. The calibration is repeated three times and the average is taken for thrust calculations. When the thruster firing is ceased, the platform displacement experiences a step-change. The magnitude of the displacement step, corresponding to the force that the thruster generates, is calculated through a linear interpolation of the readout before and after the thruster is switched off. The thrust is then obtained by multiplying calibration factor and displacement value.

The PM Halo thruster is mounted on the SSC thrust balance in the Daedalus vacuum chamber as shown in Figure 7.

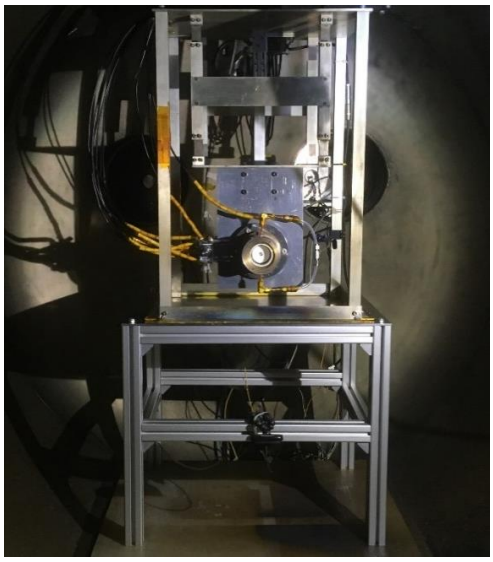

Figure 7. PM Halo Thruster Mounted on the SSC Thrust Balance in the Daedalus Vacuum Chamber.

4.2.2. Optical Emission Spectroscopy

Optical emission spectroscopy (OES) is used to investigate the plasma characteristics of the thruster plume, such as local electron temperature. For the Halo test setup, the light emitted from the plasma plume is collimated through a lens (Ocean optics 74-series), placed perpendicular to the thruster symmetry axis downstream the thruster exit, to monitor the near-field plume region. The intensity of the emission spectrum is detected by a spectrometer (Ocean Optics HR4000CG-UV-NIR) using an integration time of 0.5s.

SSC has implemented a MATLAB routine incorporating a collisional-radiative model with a set of cross-sections to simulate the main xenon emitting lines and estimate plasma properties from the measured optical emission spectra. The collisional-radiative model follows the framework presented by [7]. Figure 8 shows an example of the computed 823/828nm lines intensity ratio as function of electron temperature. The simulation represents the test case of a HET, with an acceleration voltage of 300V, at which ion collision excitation cross sections have smooth variation, and doubly charged ion signals are significantly weaker. The model input has been tailored to the case of the Halo thruster and used to estimate the space averaged electron temperature by processing the experimental intensity ratio of xenon 823nm and 828nm lines.

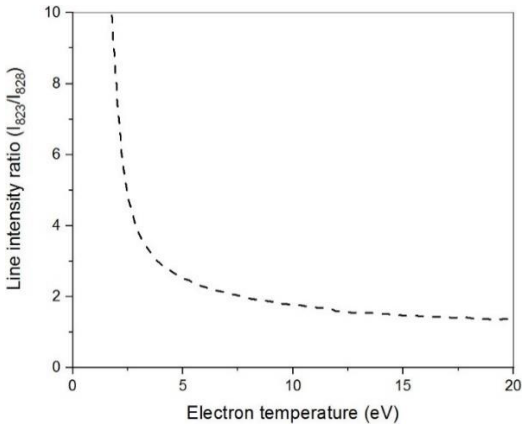

Figure 8. The line intensity ratio plot from the collisional radiative model in [7].

4.2.3. Discharge Current Waveform

Measurements of the discharge current are useful to quantify plasma oscillations and instabilities. A high frequency current probe (Hioki 3273-50) with a bandwidth of 50MHz is attached to the anode power line near the high voltage power supply to record discharge current waveforms. The probe is used to evaluate the frequency discharge current oscillations for different mass flow rates and operating conditions. Precisely, low frequency discharge current oscillations (5-35kHz) are related to ionization processes and correspond to the so-called “breathing mode”, well-known in HET [8].
Previous tests highlighted that Halo thruster shows breathing mode oscillations with peak-to-peak current as large as 6A. The period of the waveforms is comparable to the neutral residence time of xenon atoms in the discharge channel, which is around 70μs at an anode/wall temperature of 700K [5].

4.2.4. ExB probe

An ExB probe, or Wien filter, is a band-pass ion filter that employs crossed electric and magnetic fields to select ions according to their velocities. The device consists of three main regions: a collimator, the ExB field region, where an E-field is applied perpendicular to a B-field, and a drift tube where an ion collector is placed.
The Wien filter, designed at SSC, takes advantage of the constant magnetic field established by two N52 Neodymium PM, while the electric field is created by biasing two parallel electrode plates.

The charged particles enter through the collimator along a direction perpendicular to E and B-field and travel to the ExB field region. Here, the particles motion is described by the Lorentz force as in Eq.2:

$$\boldsymbol{F} = eZ(\boldsymbol{E} + \boldsymbol{u} \times \boldsymbol{B}) \qquad \text{Eq.2}$$

Where e is the elementary charge, Z the charge number, $\boldsymbol{u}$ is the particle velocity.
The ions, that reach the ion collector after the ExB region and at the end of the drift tube, are the ones undeflected by the force in the ExB field region. Therefore, the motion of these particles can be evaluated by setting Eq.2 equal to zero yielding to the following ion velocity, u_W, in Eq.3:

$$u_W = E/B = V/Bd \qquad \text{Eq.3}$$

Where V is the electrical potential established between the two electrode plates and d is the distance gap between them. Since d and B are constant, the ion velocity is proportional to the applied potential. The sweep of the plate voltage and the simultaneous monitoring the ion current, that passes through the probe using a picoammeter, generates a current-voltage characteristic related to the ion velocity distribution function. As the velocity of multicharged ions in the plasma plume is proportional to the square root of their charge state [9], the current-voltage profile allows for the identification of different ion species and their relative fractions.
An exploded view of the SSC ExB probe is presented in Figure 9.

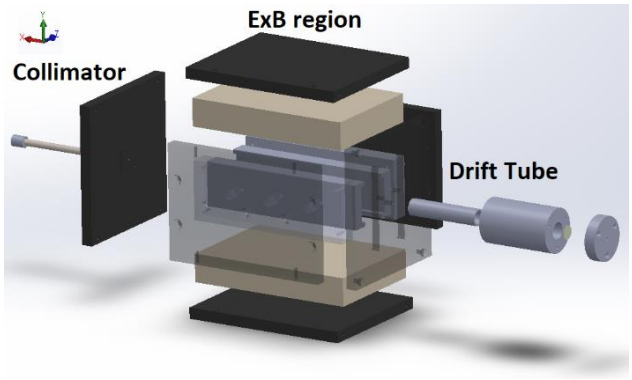

Figure 9. Exploded view of the SSC ExB probe CAD.

The external box is made of 10mm thick iron, covered by graphite foils, to allow the closure of the magnetic field lines with negligible magnetic field leaks and avoid interferences and damages caused by the plasma plume. Two Al bodies are used to separate the 150mm long and 100mm wide N52 magnets and to align the two electrode plates. The latter have a “C” shape to reduce border effect and keep uniform potential drop along the E-field direction. Since the design of the entrance collimator and the drift tube are critical to determine the resolution of the instrument [10], they were manufactured as adaptable parts. In particular, the entrance collimator is composed by three elements: a cap that can be screwed on the collimator tube to change the size collimator input orifice, the collimator tube and a plate attached to the probe external case, which determines the size of the collimator exit orifice. A similar concept is applied to the drift tube, which is encased in a cylindrical Delrin case which determines the dimensions of the input and exit apertures. Moreover, the Delrin case insulates the ion collector made of a tungsten plate.

4.2.5. Faraday probe

A Faraday probe is used to analyse the ion flux in the plasma plume. This measurement is useful to quantify thruster performance loss mechanisms and global beam properties. Based on the design guidelines in [11], the Faraday probe designed at SSC consists of a nude Faraday probe with a guard ring (Figure 10).
The collector and the guard ring are made of high purity Molybdenum, because of its low sputter yield and low secondary electron emission (SEE) properties. The collector has a diameter of 20mm and it is 10mm thick. The gap width between the collector and the guard ring is 0.3mm. The guard ring outer diameter is 30mm. It is isolated from the collector by using an isolator made of BN. The isolator is composed by two parts for easier manufacturing and to include vent holes in the ceramic base which can reduce the build up of neutral particles into the collector-guard ring gap. Moreover, fasteners passing through the isolator and the metallic parts enable to correctly align the components and are used as attachment points for electrical connections.

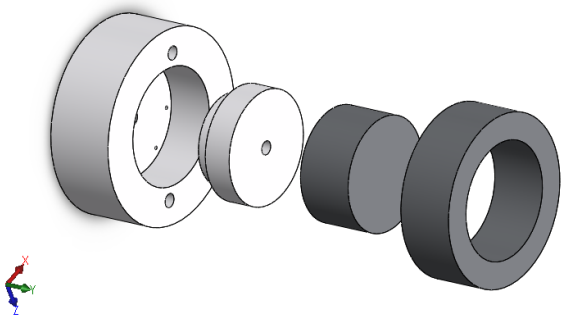

Figure 10. Exploded view of the SSC Faraday probe CAD.

5. HALO THRUSTER TEST CAMPAIGN

The Halo thruster experimental activities, previously planned for 2020, were postponed to Spring 2021 due to the COVID-19 pandemic. Performance data of the HALO thruster collected during previous test campaigns are here compared for a broad range of operating conditions and configurations.
Precisely, thruster performances are evaluated for different values of:
- Anode mass flow rate;
- Anode power;
- HCN position and orientation;
- Grounding scheme;
- Setup configurations.

The cathode and the thruster head are electrically isolated from vacuum chamber ground and floated during the measurements. In the setup with externally mounted HCN, an additional central electrode is located into the 13 mm-diameter cavity along the symmetry axis of the thruster. The central electrode is made of a molybdenum cylinder and it is either floated or grounded, to examine its effects on the thruster performance.
In particular, the following configurations are considered:
- Configuration A: Externally mounted HCN at 90° (parallel to the thruster axis – farthest point from thruster head) with floating central electrode;
- Configuration B: Externally mounted HCN at 45° (closest point from thruster head) with floating central electrode;
- Configuration C: Externally mounted HCN at 45° (closest point from thruster head) with grounded central electrode;
- Configuration D: Centrally mounted HCN.

Precisely, within the experimental campaign with externally located HCN, the cathode is mounted with the cathode orifice approximately 100mm away from the thruster centreline.
In Configuration D, the HCN is held by a metallic plate connected to the cathode base and a cap made of Macor for the cathode keeper. The purpose of the ceramic cap is twofold. First, it maintains the position of the cathode on the central axis by directing neutral gas flow coming from the cathode into the thruster discharge channel. Second, it protects the keeper from possible ion bombardment, which can cause sputtering erosion of the keeper decreasing lifetime of the cathode. The tests are performed by using a COTS HCN, as the OSMO cathode will be introduce in the next test campaign. High purity xenon gas is used as propellant for both the anode and the hollow cathode. The propellant mass flow is regulated using xenon mass flow controllers (Bronkhorst, 10 sccm full range, calibrated by the manufacturer) with a maximum uncertainty of 0.002mg/s.
During most of the tests, the cathode mass flow rate (0.29mg/s), cathode heater current (15A), and cathode keeper current (1.5A) is kept constant. The anode mass flow rate ranges between 0.59 and 1.18mg/s in the externally-mounted HCN configuration. In the centrally-mounted HCN setup, only 0.10mg/s Xe is necessary to sustain the discharge. The anode voltage lowest value is 150V and is increased up to 300V, resulting in an anode power between about 50 and 400W. Background pressure (corrected for xenon) is measured by an ion gauge (Edwards AIM-S-NW25). The maximum background pressure is $1.3 \cdot 10^{-4}$Torr at 1.18mg/s anode mass flow rate and 0.29mg/s cathode mass flow rate.

6. Performance Result Comparison

The thrust and the anode specific impulse are plotted as function of the anode voltage for Configuration A (Figure 11), B (Figure 12) and C (Figure 13). Figure 14 illustrates the total specific impulse, whose estimation includes the total of the cathode and anode mass flow rate, for Configuration D. The configurations were previously described in Sec. 5.

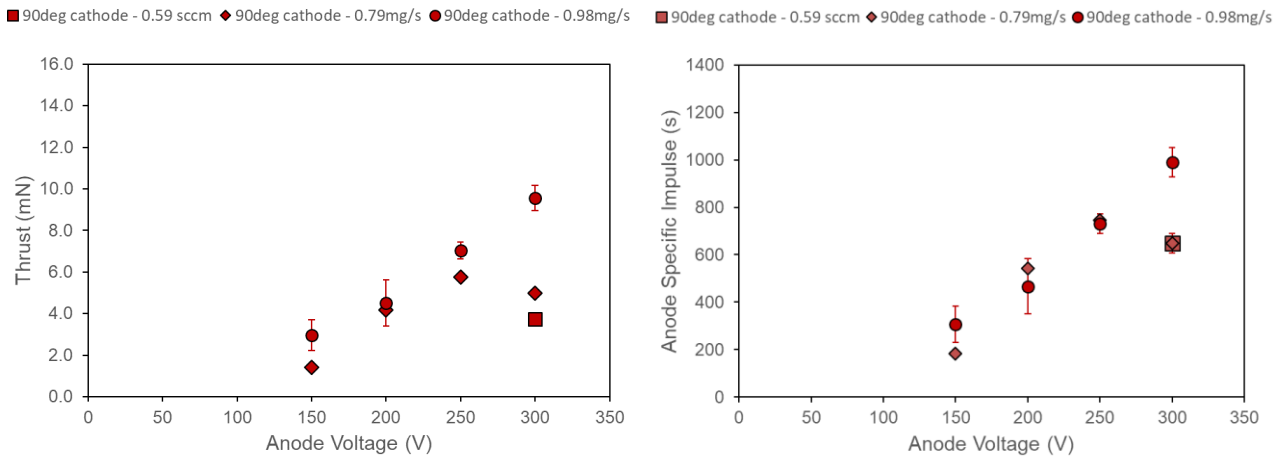

Figure 11. Thrust and Anode Specific Impulse results for Configuration A. Anode mass flow rate of 0.59, 0.79, 0.98 mg/s.

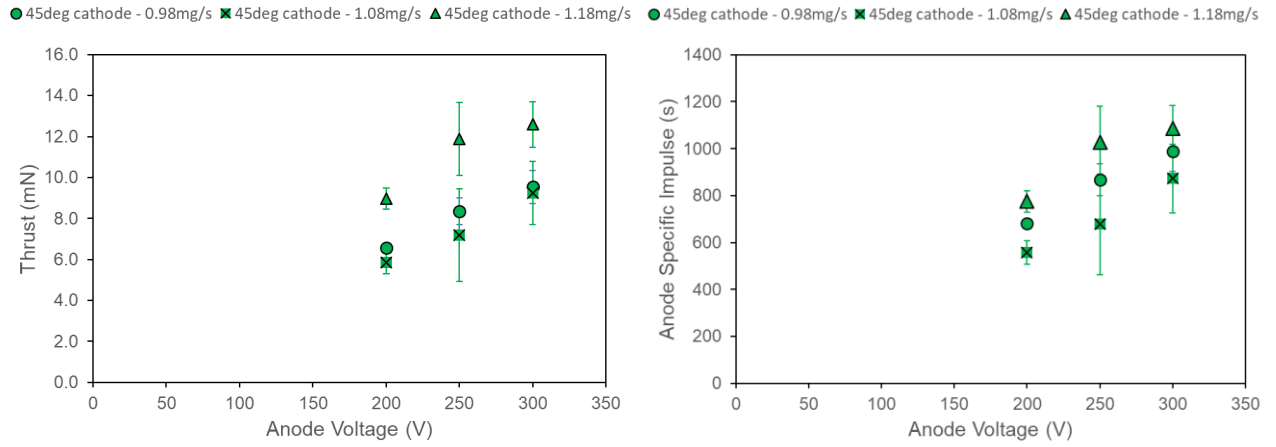

Figure 12. Thrust and Anode Specific Impulse results for Configuration B. Anode mass flow rate of 0.98, 1.08, 1.18 mg/s.

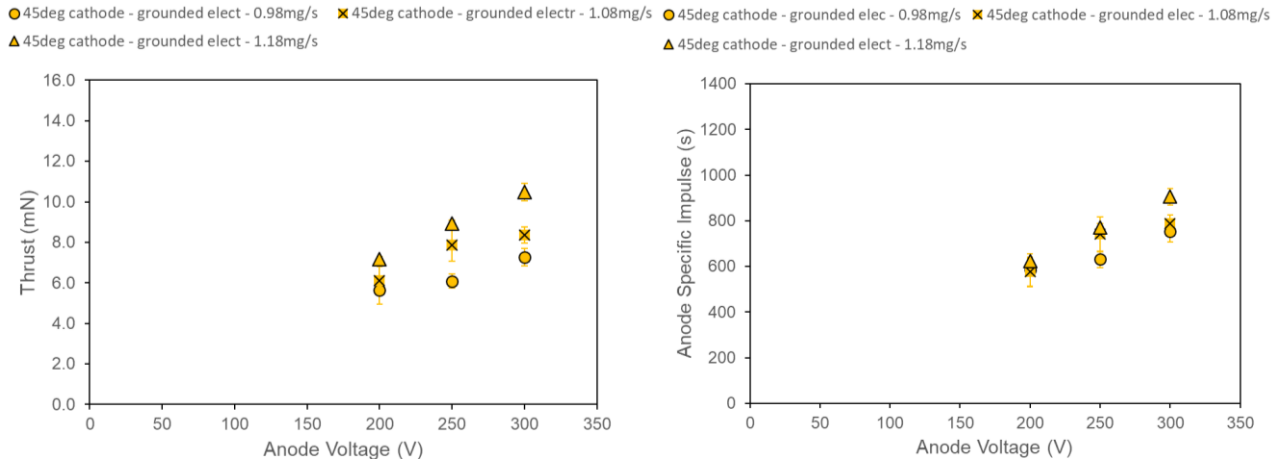

Figure 13. Thrust and Anode Specific Impulse results for Configuration C. Anode mass flow rate of 0.98, 1.08, 1.18 mg/s.

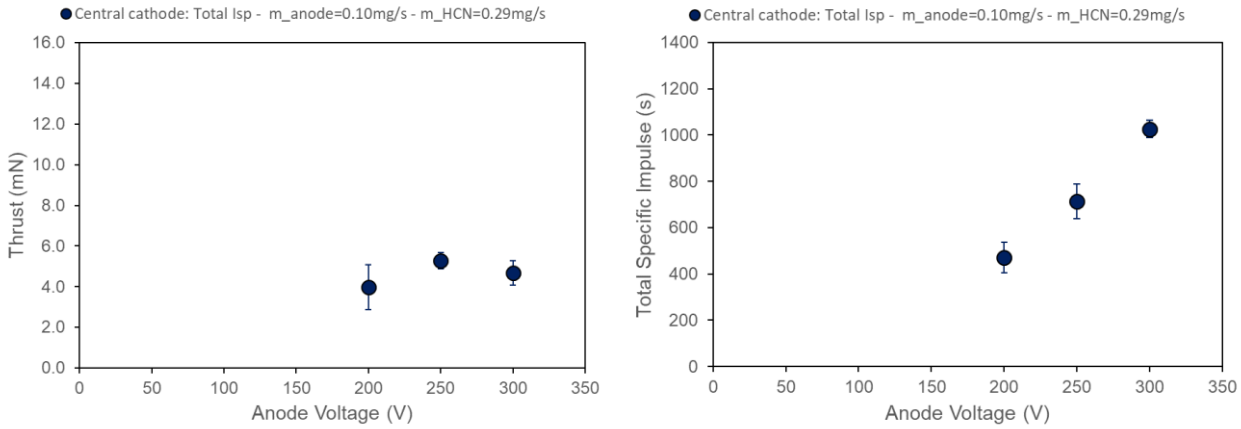

Figure 14. Thrust (on the left-hand side) and Specific Impulse (on the right-hand side) results for Configuration D: I_{sp} is evaluated as total specific impulse: Anode mass flow rate is 0.10 mg/s, cathode mass flow rate is 0.29 mg/s. Note that in this configuration, the total specific impulse is the most appropriate metric since the cathode propellant flow is recovered within the thruster channel.

During this experimental campaign, the thrust measurement at each operating condition is repeated three times; the plots report the mean, as the central point, and the standard deviation, in form of double-sided error bar.

The thrust monotonically increases with discharge voltage and anode mass flow rate, while the anode specific impulse increases with increasing discharge voltage. The average thrust values for the floating central electrode configuration at 45° (Configuration B) ranges from 5.9 to 12.6mN at discharge powers of 185 to 380W translating to anode efficiencies of 8-25%. The thrust presents a sensible decrease (up to 25%) when the central electrode is grounded (Configuration C).

Figure 15 shows a comparison between the values of the discharge current as a function of the anode voltage between Configuration A (in red), Configuration B (in green) and Configuration C (in yellow) for three mass flow rates: 0.98 mg/s (circle marker), 1.08 mg/s (square marker), 1.18 mg/s (triangular marker). The discharge current increases slightly for the grounded central electrode configuration compared to the floating central electrode one. The difference in thrust between Configuration B and C is too large to be explained with the 1-3% increase in the discharge current. Moreover, the cathode-to-ground voltage varies between -28 to -32 V, and there is no significant difference between both configurations. A possible explanation originates from the different plasma potential distribution in the discharge channel with a decrease of the axial electric field. Increased secondary electron emission may lower the total electron temperature in the discharge channel, enhance the cross-field electron transport by modifying the sheath potential, and limit the maximum achievable electric field in the magnetized plasma.

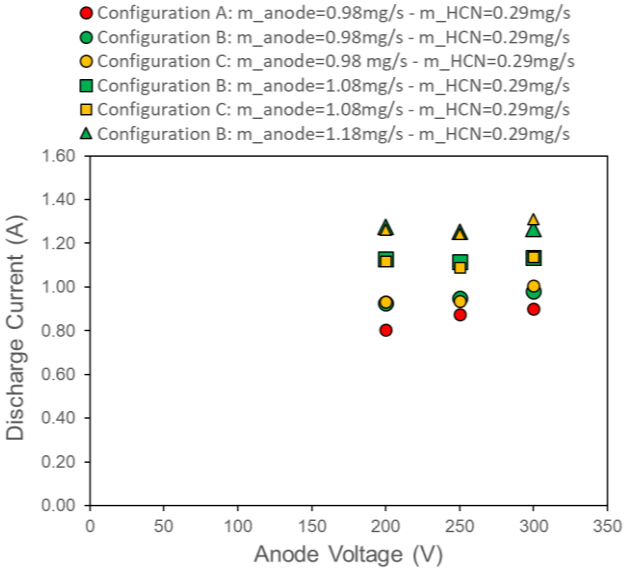

Figure 15. Discharge current comparison between Configuration A (red), Configuration B (green) and Configuration C (yellow) for three mass flow rates: 0.98 mg/s (circle marker), 1.08mg/s (square marker), 1.18 mg/s (triangle marker).

It is useful to mention that the different configurations of the PM Halo are evaluated by feeding the HCN at the same mass flow rate of 0.29mg/s, whereas the minimum anode mass flow rate was 0.59mg/s for Configurations A, 0.98mg/s for Configurations B and C. Configuration D allows operation at significantly lower anode mass flow rate of 0.10 mg/s, thanks to the recovery of the cathode propellant flow.

The total specific impulse for the different PM Halo thruster configurations is compared in Figure 16 at the lowest total mass flow rate for which the thruster operation was stable for each configuration.

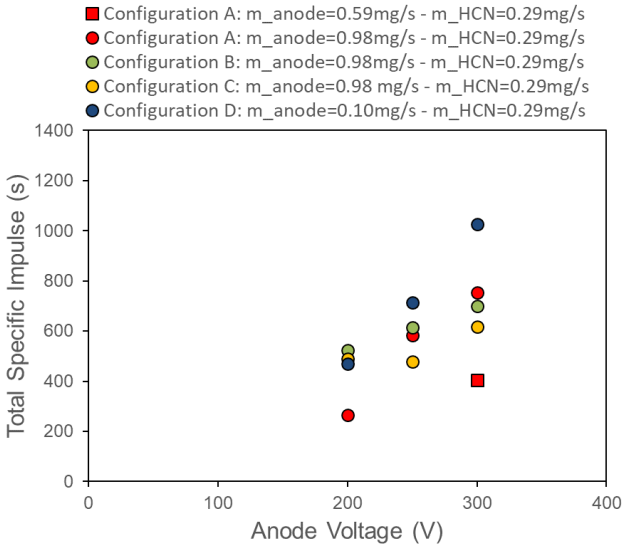

Figure 16. Total specific impulse: PM Halo thruster configurations are compared at the lowest total mass flow rate at which the thruster operation was stable.

Figure 17 shows a photo of PM Halo thruster with centrally mounted HCN (Configuration D) during the previous test campaign in Daedalus vacuum chamber at SSC Electric Propulsion Laboratory. The test matrix for the campaign on the PM Halo in Configuration D initially included a broader range of test points encompassing the mass flow rate interval used in the other configurations, however this further investigation was inhibited by the need to upgrade multiple features of the experimental setup that will be ready for the 2021 test campaign. Moreover, the use of this specific cathode model yields a cathode-to-anode flow rate ratio significantly higher than that of typical flight model thrusters, therefore the results and conclusions, achieved during the test campaign, are valid for the specific operating conditions of this cathode only.

Figure 17. Photo of PM Halo thruster in Configuration D (centrally- located cathode) - Daedalus vacuum chamber, SSC Electric Propulsion Laboratory, University of Surrey.

A complete comparison between the different Halo models includes the analysis of the PM and EM design performances. For this purpose, Figure 18, Figure 19 and Figure 20 compare PM Halo thruster in Configuration B with a 5-cm channel diameter Halo thruster laboratory model with EMs. In both prototypes, the hollow cathode is externally mounted. As shown in Figure 19, the PM prototype demonstrates higher thrust-to-power ratios, while (Figure 18) the EM coil version provides higher anode specific impulses. In terms of efficiency (Figure 20), PM Halo reaches the highest anode thrust efficiency at 0.98mg/s and 1.18mg/s anode mass flow.

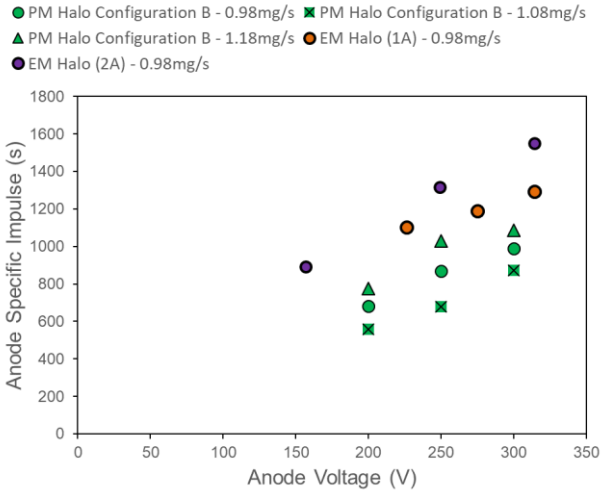

Figure 18. Anode specific impulse as function of the anode voltage: PM Halo (Configuration B) is indicated with green markers at 0.98mg/s (circle marker), 1.08 mg/s (square marker), 1.18 mg/s (triangle marker); EM Halo with circle markers at 0.98 mg/s and EM current of 1A (orange), at 0.98 mg/s and EM current of 2A (violet).

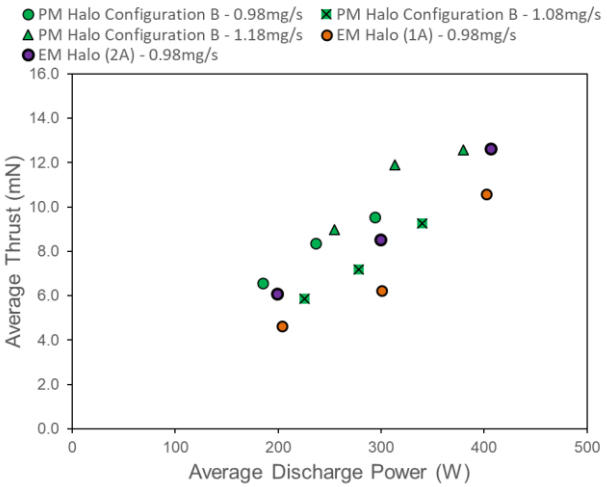

Figure 19. Thrust-to-power ratio: PM Halo (Configuration B) is indicated with green markers at 0.98mg/s (circle marker), 1.08 mg/s (square marker), 1.18 mg/s (triangle marker); EM Halo with circle markers at 0.98 mg/s and EM current of 1A (orange), at 0.98 mg/s and EM current of 2A (violet).

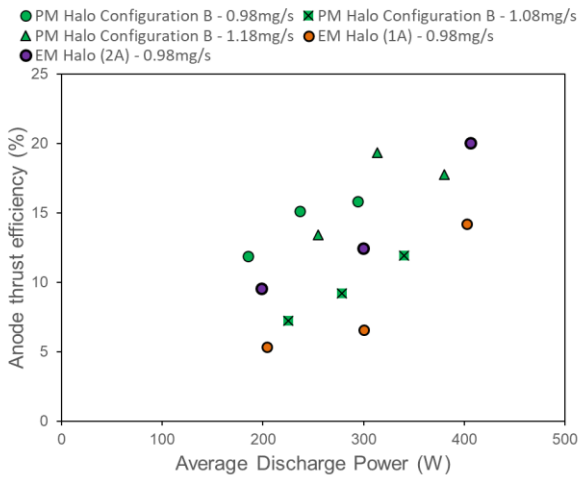

Figure 20. Anode thrust efficiency as function of the discharge power: PM Halo (Configuration B) is indicated with green markers at 0.98mg/s (circle marker), 1.08 mg/s (square marker), 1.18 mg/s (triangle marker); EM Halo with circle markers at 0.98 mg/s and EM current of 1A (orange), at 0.98 mg/s and EM current of 2A (violet).

7. CONCLUSIONS

The Halo thruster is a novel propulsion system based on the electrostatic acceleration of propellant ions, produced in a magnetised plasma discharge, characterized by a closed-loop electron drift which is sustained by the combination of electric and magnetic fields. The B-field, generated by two concentrically aligned SmCo annular PMs, is designed to include magnetic null regions: a downstream null point near the channel exit and an upstream halo in front of the anode. When compared with EM coils of the same dimensions, the use of PMs is advantageous in terms of power consumption, heat dissipation and design simplification. Moreover, the high B-field strength at small scale could promote better plasma confinement, reducing wall sputtering erosion caused by high-energy ions and decreasing power loss associated to plasma flows to the channel walls.

The OSMO cathode, a HCN based on LaB_6 emitter and molybdenum keeper electrode, was recently developed at SSC and is going to be implemented as Halo thruster neutraliser. The HCN is assembled at the bottom end of the cylindrical discharge channel with its axis aligned to the thruster centreline. This configuration enables to use the whole propellant supplied to the thruster to generate thrust, improves coupling of the cathode plume with the thruster discharge and promotes near-field plume symmetries. Furthermore, this design allows to keep a low electrostatic potential along the magnetic field line, overlapping with thruster centreline and creating a convergent field, which can reduce plume divergence.

In Spring 2021, a test campaign at SSC Electric Propulsion laboratory is going to investigate PM Halo plasma plume characteristics and thruster performances. A novel experimental setup in SSC Daedalus vacuum chamber comprises a hanging pendulum-type thrust stand, OES, a high frequency current probe for plasma oscillation quantification and newly developed ExB and Faraday probes.

Previous research activities have characterized the performances of the PM Halo thruster models in different cathode configurations. The tests have confirmed the possibility to operate Halo with a centrally mounted cathode. In this configuration, preliminary data have demonstrated that thrust and thrust-to-power ratio are lower in comparison to the Halo configurations with the external cathode and operating in the same power range. A sensible propellant saving was observed, as PM Halo with central cathode demonstrated stable firing conditions at 0.10 mg/s of Xe anode mass flow rate, in comparison with a minimum of 0.59 mg/s Xe for the same cathode mass flow rate of 0.29 mg/s for the externally-mounted configuration. Moreover, the total specific impulse (accounting for anode and cathode mass flows) of the PM Halo with centrally-located cathode showed an increase of more than 15% at the anode potential of 250 V and about ~40% at 300 V in comparison with the Configuration A (anode flow 0.59 mg/s), B (anode flow 0.98 mg/s) and C (anode flow 0.98 mg/s) with externally-mounted cathode. Note that it was not possible to perform comparisons at the same anode flow settings due to the different operating envelopes of the thruster in the different configurations.

Finally, a comparison with a 5cm diameter EM Halo prototype suggested that, in general, the PM Halo version reached a higher thrust-to-power ratio, while the EM version provided a higher anode specific impulse.

8. ACKNOWLEDGMENTS

The Halo thruster research and development activities are supported by Airbus Defence & Space and the UK Space Agency under the “Development of a Halo-200 Electric Propulsion System” project.

9. REFERENCES

1. Y. Raitses, N.J. Fisch, “Parametric Investigations of a Nonconventional Hall Thruster”, Physics of Plasmas, 8(5), 2579-2586.

2. D. G. Courtney and M. Martınez-Sanchez, “Diverging Cusped-Field Hall Thruster (DCHT).”, 30th International Electric Propulsion Conference (IEPC), 2007.

3. B. Karadag, S. Cho, I. Funaki, Y. Hamada, and K. Komurasaki, “External discharge plasma thruster,” J. Propul. Power, 2018.

4. A. Lucca Fabris, T. Wantock, A. Gurciullo, R. Moloney, A. Knoll, T. Potterton, P. Bianco, “Overview of Halo thruster research and development activities”, Space Propulsion Conference Proceedings, 2018.

5. B. Karadag, S. Masillo, R. Moloney, A. Lucca Fabris, T. Potterton, A. Knoll, P. Bianco. “Experimental Investigation and Performance Optimization of the Halo thruster”, 36th International Electric Propulsion Conference (IEPC), 2019.

6. T.G. Wantock. “Thrust Balance Performance Characterisation and Internal Langmuir Probe Plasma Diagnostics for a Halo Thruster”. PhD Dissertation, University of Surrey, UK - 2017.

7. Dressler, R. A., Y. Chiu, O. Zatsarinny, K. Bartschat, R. Srivastava, L. Sharma, “Near-Infrared Collisional Radiative Model for Xe plasma electro-static thrusters: the role of metastable atoms”. Journal of Physics D: Applied Physics, 42, 2009.

8. Boeuf J. P., Garrigues L., “Low frequency oscillations in a stationary plasma thruster,” J. Appl. Phys. 84, 3541, 1998.

9. Rohit Shastry, Richard R. Hofer, Bryan M. Reid, and Alec D. Gallimore, “Method for analyzing ExB probe spectra from Hall thruster plumes”, Rev. Sci. Instrum. 80, 063502, 2009.

10. A. Gurciullo, “Electric propulsion technologies for enabling the use of molecular propellants”. PhD Dissertation, University of Surrey, UK – 2018

11. Daniel L. Brown, Mitchell L. R. Walker, James Szabo, Wensheng Huang, John E. Foster, “Recommended Practice for Use of Faraday Probes in Electric Propulsion Testing”, J. Propul. Power, 2016.